Catalysis Science & Technology

Accepted Manuscript

This article can be cited before page numbers have been issued, to do this please use: Y. Ren, B. Wu, F. Wang, H. Li, G. Lv, M. Sun and X. Zhang, *Catal. Sci. Technol.*, 2019, DOI: 10.1039/C9CY00401G.

ROYAL SOCIETY OF CHEMISTRY

rsc.li/catalysis

Journal Name

ROYAL SOCIETY OF CHEMISTRY View Article Online
DOI: 10.1039/C9CY00401G

ARTICLE

Chlorocuprate(I) ionic liquid as an efficient and stable Cu-based catalyst for hydrochlorination of acetylene†

Yanfei Ren,[‡a] Botao Wu,[‡ab] Fumin Wang,*[a] Hang Li,[a] Guojun Lv,[a] Mingshuai Sun,[a] Xubin Zhang*[a]

Received 00th January 20xx,
Accepted 00th January 20xx

DOI: 10.1039/x0xx00000x

www.rsc.org/

The gas-liquid reaction process for acetylene hydrochlorination, especially using ionic liquids (ILs) as the homogeneous reaction medium, has gained more attention because it can effectively avoid the deactivation caused by hot spots and carbon deposition. However, the relatively low activity and high price of the currently used ILs limit their practical applications. Herein, we synthesize a series of chlorocuprate(I) ILs to explore an efficient and stable Cu-based catalyst for acetylene hydrochlorination. N-methylpyrrolidonium hydrochloride-0.60CuCl ([Hnmpo]Cl-0.60CuCl) IL obtain the best catalytic performance, showing the acetylene conversion of 86% over 150 h at the conditions of 180 °C and 50 h^{-1} GHSV. It is confirmed that Cu(I) species is the major active component and extremely stable under the reaction conditions *via* characterizations of TGA-DSC-FTIR, ICP-OES, XPS, UV-Vis, ESI-MS, and Raman. In addition, [Hnmpo]Cl-0.60CuCl IL has the capacity to effectively activate HCl, which is directly observed by *in situ* FTIR. By combining experiment results and theoretical calculations, we propose the reaction mechanism and find that the catalytic performance of chlorocuprate(I) ILs is positively correlated with the adsorption of HCl. The strong interaction with HCl is identified as the key characteristic of [Hnmpo]Cl-CuCl IL, which endows it with excellent catalytic performance. Briefly, this study shows that the cost-effective [Hnmpo]Cl-CuCl IL can be a viable alternative to the commercial heterogeneous $HgCl_2$/AC catalyst for acetylene hydrochlorination.

1. Introduction

Vinyl chloride monomer (VCM) is an essential material for the synthesis of polyvinyl chloride (PVC), which is the third most widely used plastic material in the world. Acetylene hydrochlorination, originally started in the 1930s, is still applied for industrial VCM production in the countries where acetylene can be obtained economically from abundant coal.[1] At present, activated carbon (AC) supported 10–15 wt% mercuric chloride is extensively used as industrial catalyst in acetylene hydrochlorination.[2] Nevertheless, the toxic mercury chloride catalyst has encountered a number of shortcomings, such as the loss of active components due to the hot spots in fixed bed reactors, as well as the environmental disruptions associated with the catalyst preparation, application and disposal. Moreover, based on the requirements of the Minamata Convention,[3] the use of mercury will be forbidden in the future. Hence, one of the priorities of acetylene-based PVC industry is the development of environmentally friendly non-mercury catalysts.

Up to now, following the pioneering work of Hutchings,[4-8] studies on non-mercury catalysts for acetylene hydrochlorination chiefly concentrate on precious metal catalysts, especially Au-based catalysts. A lot of efforts have been made to minimize the cost of Au-based catalysts by decreasing the Au loading or increasing the stability.[9-11] However, its high price is still the major obstacle to the low value-added PVC industry.[12] To meet economic benefits, non-precious metal catalysts have gained more attention in recent years.[13-18] Cu-based catalysts are generally studied because of their relatively good catalytic activity.[13-16] Nevertheless, almost all Cu-based catalysts still suffer from low activity and severe deactivation. Thus, it is a challenge to improve the activity and the long-term stability of Cu-based catalysts for acetylene hydrochlorination.

In order to solve this problem, some researchers turn their attention to the gas-liquid reaction process, which can give efficient temperature control and heat removal compared to the gas-solid reaction.[19-21] And the active component would be better developed in a homogeneous reaction medium.[22, 23] In consequence, the gas-liquid reaction could effectively avoid the disadvantages of solid catalysts, like the hot spot, the surface coke deposition, and the pulverization of AC. Currently, due to the extraordinary physicochemical properties such as negligible vapor pressure, good solubility and high thermal stability, ionic liquids (ILs) have attracted remarkable attention for applications in the gas-liquid reaction of acetylene hydrochlorination.[19-21, 24] Qin *et al.* proved the gas-liquid reaction for acetylene hydrochlorination using IL as reaction

[a] School of Chemical Engineering and Technology, Tianjin University, Tianjin 300350, P. R. China. E-mail: wangfumin@tju.edu.cn (F. Wang), tjzxb@tju.edu.cn (X. Zhang)
[b] Key Laboratory of Bioorganic Chemistry and Molecular Engineering, Ministry of Education and Beijing National Laboratory for Molecular Science, College of Chemistry and Molecular Engineering, Peking University, Beijing 100871, P. R. China
‡ Equal contribution
† Electronic Supplementary Information (ESI) available. See DOI: 10.1039/x0xx00000x

medium and metal chloride as active component, and found [Bmim]Cl had the highest activity among different ILs.[19] Hu *et al.* prepared a metal nanoparticles/anionic surfactant IL system, and the Pd NPs/[P_{4444}][C_{17}COO] showed excellent catalytic activity.[20] Later, Yang *et al.* reported a Pd NPs@[P_{4444}][C_{17}COO]-C_{14} liquid-liquid biphasic system, which exhibited better catalytic performance than the Pd NPs/[P_{4444}][C_{17}COO].[21] Very recently, Zhou *et al.* proposed the use of 1-alkyl-3-methylimidazolium-based ILs as single component metal-free catalysts.[24] Overall, using ILs as reaction medium not only provides an environmentally friendly choice for gas-liquid reaction but also can achieve better catalytic performance. For instance, the presence of ILs might activate the reactant gas and effectively stabilize the oxidized metal complex,[22, 23, 25] thereby improving its catalytic efficiency. However, the high cost of the present used ILs, such as imidazolium and quaternary phosphonium salts, greatly restricts their sustainable applications in PVC industry. Hence, it still remains huge demand to develop a low-cost IL catalytic system.

By directly mixing of a metal chloride and an organic halide salt, it is possible to synthesize a halometallate IL with very interesting and useful properties. Currently, halometallate ILs have received increasing interest as novel catalysts in a broad range of reactions.[26-28] Supported halometallate ILs catalysts have also been used in acetylene hydrochlorination,[22, 23, 29] such as Au(III)-[Prmim]Cl/AC,[22] Ru(III)-ChCl/AC,[29] and Pd(II)-[Bmim]Cl/AC.[23] To the best of our knowledge, Cu(I) species as the active component has not been successfully used in the acetylene hydrochlorination because of its unstable property, which could lead to rapid deactivation. Surprisingly, Cu(I) species could remain stable in IL,[30, 31] which enlightened us to find a chlorocuprate(I) IL with higher catalytic activity and significant price advantage over the currently used ILs. Herein, for the first time, we prepared a series of chlorocuprate(I) ILs and tested their catalytic performance in a continuous gas-liquid process for acetylene hydrochlorination. N-methylpyrrolidonium hydrochloride-0.60CuCl ([Hnmpo]Cl-0.60CuCl) IL was found to have remarkable catalytic performance and long-term stability. Besides, the IL was investigated by various characterizations to uncover the properties of the active component. Furthermore, based on our experimental results and theoretical calculations, we proposed the possible mechanism and correlated the catalytic performance with the adsorption of HCl and C_2H_2. We believe that the encouraging results of this work would help the development of Cu-based catalysts for acetylene hydrochlorination.

2. Experimental

2.1. Materials

Cuprous chloride (CuCl, purity 97%) was purchased from Shanghai Meryer Chemical Technology Co., Ltd. Hydrogen chloride (HCl, purity > 99.99%) and acetylene (C_2H_2, purity > 99.99%) were purchased from Tianjin Huanyu Gas Co., Ltd. Choline chloride (ChCl, purity ≥ 98%), 1-butyl-3-methylimidazolium chloride ([Bmim]Cl, purity ≥ 99%), tetrabutylphosphonium chloride ([P_{4444}]Cl, purity ≥ 96%), tetrabutylammonium chloride ([N_{4444}]Cl, purity ≥ 98%), triethylamine hydrochloride ([Et_3NH]Cl, purity ≥ 99%), and pyridine hydrochloride ([PyH]Cl, purity ≥ 98%) were purchased from Shanghai D&B Chemical Technology Co., Ltd. N-methylpyrrolidinone (NMPO, purity > 99.5%), 1-methylimidazole (purity 99%), and N-methylpyrrolidine (purity 98%) were purchased from Shanghai Macklin Biochemical Co., Ltd. Hydrochloric acid (aqueous solution, 36–38 wt%) was purchased from Tianjin Yuanli Chemical Co., Ltd. All the materials were used without further purification.

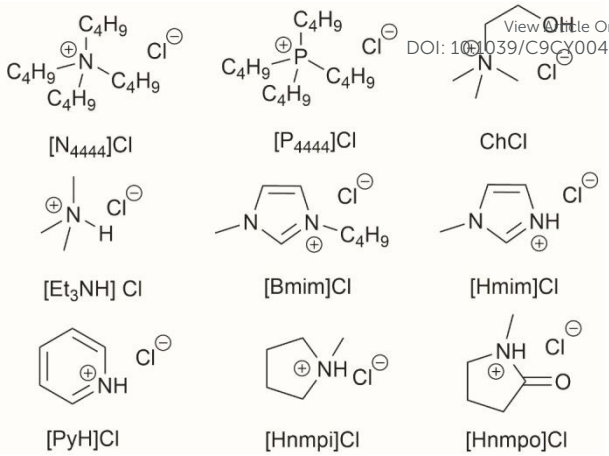

Fig. 1 The molecular structure of the nine organic chloride salts.

2.2. Preparation of organic chloride salt

1-methylimidazolium hydrochloride ([Hmim]Cl), N-methylpyrrolidonium hydrochloride ([Hnmpo]Cl) and N-methylpyrrolidinium hydrochloride ([Hnmpi]Cl) were synthesized according to the previous literature.[32] Hydrochloric acid was added dropwise to 1-methylimidazole over a period of 20 min under a temperature of 0–5 °C. The mixture was stirred for an additional period of 12 h at 50 °C. Then, water was removed under reduced pressure by rotary evaporation and the white crude solid product was washed with diethyl ether to remove any unreacted starting materials. After vacuum drying overnight at 60 °C, [Hmim]Cl was obtained. The synthesis of [Hnmpo]Cl and [Hnmpi]Cl followed protocols same to the [Hmim]Cl. The purity of the three organic chloride salts was confirmed by ^{1}H NMR recorded on a Bruker AVANCE III spectrometer (Fig. S1).

2.3. Synthesis of chlorocuprate(I) IL

Chlorocuprate(I) IL was prepared by mixing CuCl with the required amount of above-mentioned organic chloride salt together under a protective atmosphere of N_2, then stirring at 100 °C for 24 h as the similar method recorded in the literature.[33] The molecular structure of nine organic chloride salts is summarized in Fig. 1. We expressed the composition of chlorocuprate(I) IL in terms of mole fraction of CuCl, x = mole of CuCl / mole of (CuCl + organic chloride salt).

2.4. Evaluation of catalytic performance

The catalytic performance of chlorocuprate(I) ILs for acetylene hydrochlorination was tested in a self-designed quartz bubbling micro-reactor, which had a diameter of 10 mm and a length of 400 mm. The temperature was controlled by a magnetic stirring oil bath with a heating height of 350 mm. The experimental setup was presented in Fig. S2.

The reactor contained 15 mL of IL and was purged with N_2 to remove water and air before the reaction. Then HCl (9.0 mL/min) was passed for 60 min. Subsequently, C_2H_2 (7.5 mL/min) was fed through the reactor with a HCl/C_2H_2 volume ratio of 1.2 to obtain an acetylene gas hourly space velocity (GHSV) of 30 h^{-1}. The long-term stability experiments were carried out with 10 mL of IL in the same apparatus. The effluent gas was analyzed online by a gas chromatograph (Benfen-Ruili, 3420A) after eliminating unreacted HCl and water.

2.5. Characterization

Gas chromatography-mass spectrometry (GC-MS) was conducted using an Agilent 5975C instrument to detect the reaction by-products.

Viscosity was measured using a Shanghai Equitable NDJ-5S rotational viscometer by a spindle no. 1 at 6 rpm, and the temperature was controlled by an external oil bath.

Thermogravimetric analysis-Differential scanning calorimetry-Fourier transform infrared (TGA-DSC-FTIR) measurement provided information about the thermal stability and decomposition products of IL, which was performed using a NETZSCH STA 449 F5 thermal analyzer coupled with a Bruker Tensor 27 FTIR spectrometer. About 15 mg of IL was heated from 40 °C to 800 °C at a heating rate of 10 °C/min under N_2 atmosphere with a flow rate of 50 mL/min. The FTIR spectra were acquired in the range from 4000 cm^{-1} to 600 cm^{-1} at a resolution of 4 cm^{-1}.

TGA was used to evaluate the coke amount, and was performed on a Mettler Toledo TGA/DSC 2 instrument under an air atmosphere with a flow rate of 30 mL/min, and the temperature increased from 30 to 800 °C at a heating rate of 10 °C/min.

X-ray photoelectron spectroscopy (XPS) was performed on a Thermo ESCALAB 250XI instrument to analyze the elemental composition of the IL and the chemical states of copper. The spectrometer was calibrated for the C 1s signal at 284.8 eV with a resolution step width of 0.1 eV, and the raw spectra were fitted using the smart function by Avantage software.

Inductively coupled plasma-optical emission spectrometry (ICP-OES) was conducted by using a Varian VISTA-MPX instrument to measure the copper content of the IL.

Electrospray ionization mass spectrometry (ESI-MS) was recorded on a Bruker Daltonics miorOTOF-QII instrument by using acetonitrile as the solvent to identify the copper species.

Raman spectra of the IL at solid state were tested by using a Renishaw inVia Reflex instrument in the range 200–800 cm^{-1} with a 532 nm argon ion laser for excitation.

Ultraviolet-visible (UV-vis) spectra were acquired with a Jasco UV 550 spectrometer in the range of 200–800 nm by adopting acetonitrile as the solvent.

In situ FTIR spectra measurement were conducted on a Mettler Toledo ReactIR 15 instrument equipped with an AgX optic fiber and a Diamond insertion probe from 2400–800 cm^{-1} by using acetonitrile as the solvent.

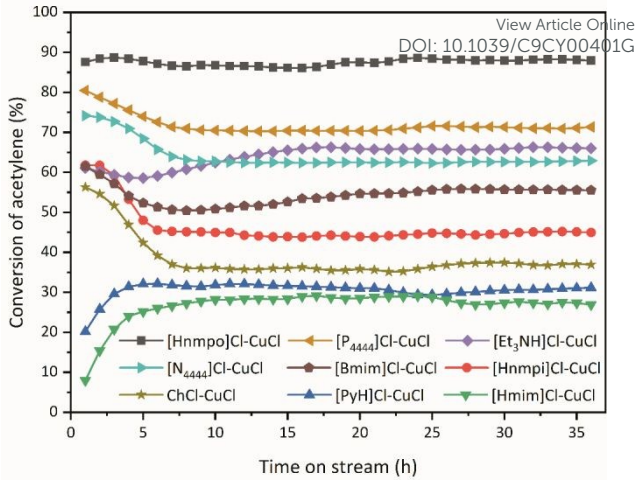

Fig. 2 Catalytic performance over different chlorocuprate(I) ILs. Reaction conditions: *x*(CuCl) = 0.67, GHSV(C_2H_2) = 30 h^{-1}, T = 160 °C, and V(HCl)/V(C_2H_2) = 1.2.

2.6. Calculation details

Geometry optimizations were performed using the Gaussian 09 package[34] at the B3LYP-D3(BJ)/6-31G**/LanL2dz level of the theory.[35-41] All of the optimized geometries were examined as stable point or transition state structures by frequency calculations. Thermal corrections, natural population analysis (NPA) were conducted at the same theory level.[42] To obtain better accuracy, energies of the optimized geometries were calculated using M06-D3/6-311+G(2df,2p)/SDD level.[43-46] The computed structures were illustrated using CYLview.[47] The analysis and visualization of calculation results were carried out by Multiwfn and VMD.[48, 49]

3. Results and discussion

3.1. Catalytic performance over different chlorocuprate(I) ILs

To make the research results more convincing, we chose a range of organic chloride salts, including the most commonly used imidazolium and quaternary phosphonium salts, to prepare chlorocuprate(I) ILs. The mole fraction of CuCl was fixed at 0.67, and the catalytic performance of each IL was evaluated at acetylene GHSV of 30 h^{-1}, temperature of 160 °C, and HCl/C_2H_2 volume ratio of 1.2 for 36 h. As shown in Fig. 2, nine different ILs exhibit diverse catalytic performance on the conversion of acetylene. To our surprise, [Hnmpo]Cl-0.67CuCl IL not only achieves the highest acetylene conversion of 88.0% at 36 h, but also has a relatively low price (Fig. S3). [P_{4444}]Cl-0.67CuCl IL has the second highest acetylene conversion, but it encounters the shortcoming of high price. Besides, [Bmim]Cl-0.67CuCl IL only achieves the conversion of acetylene to 55.5%. Compared with

View Article Online
DOI: 10.1039/C9CY00401G

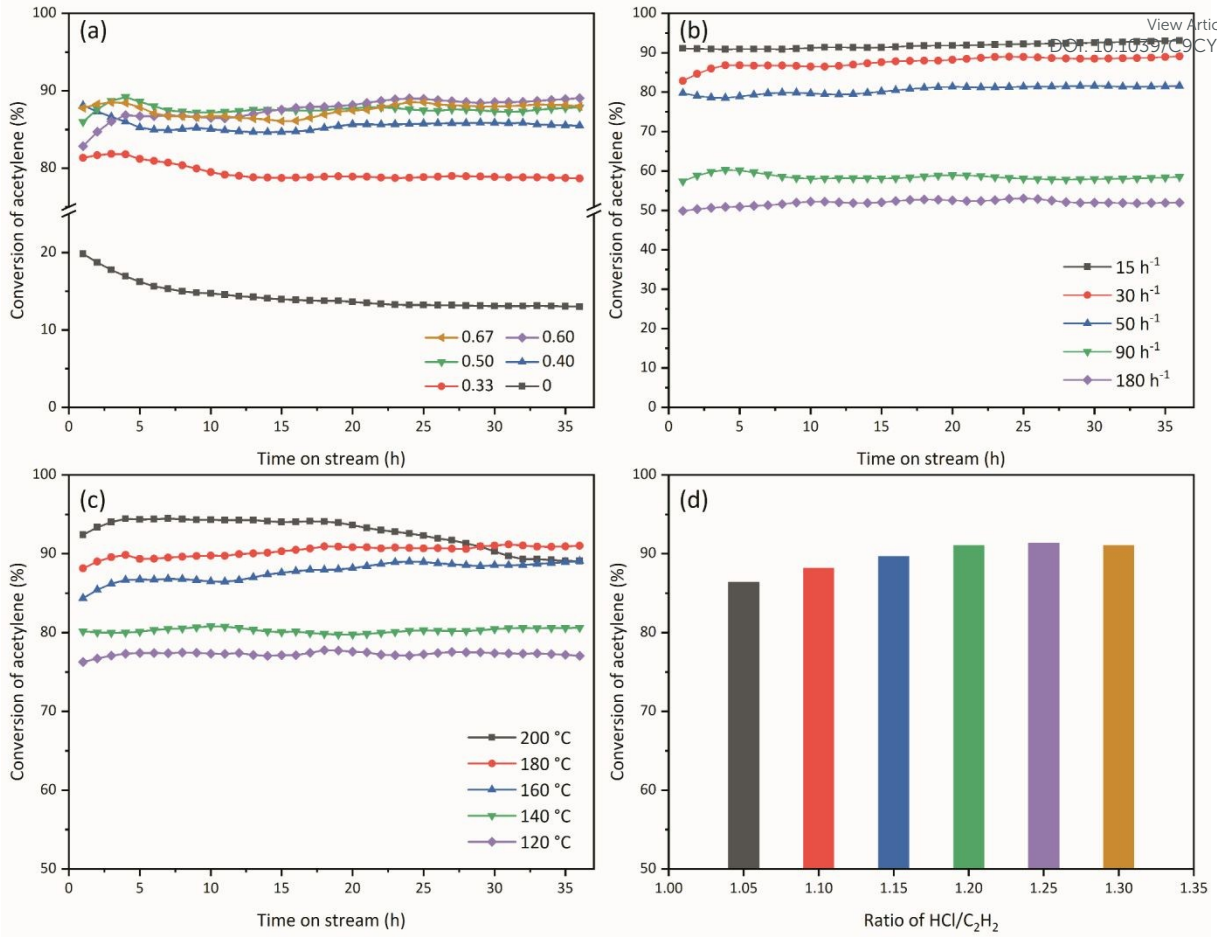

Fig. 3 Catalytic performance of [Hnmpo]Cl-CuCl IL for acetylene hydrochlorination. (a) Effect of CuCl mole fraction. Reaction conditions: GHSV(C_2H_2) = 30 h^{-1}, T = 160 °C, and V(HCl)/V(C_2H_2) = 1.2. (b) Effect of acetylene GHSV. Reaction conditions: *x*(CuCl) = 0.60, T = 160 °C and V(HCl)/V(C_2H_2) = 1.2. (c) Effect of reaction temperature. Reaction conditions: *x*(CuCl) = 0.60, GHSV(C_2H_2) = 30 h^{-1} and V(HCl)/V(C_2H_2) = 1.2. (d) Effect of HCl/C_2H_2 volume ratio. Reaction conditions: *x*(CuCl) = 0.60, GHSV(C_2H_2) = 30 h^{-1} and T = 180 °C.

[Hnmpo]Cl, since [Hnmpi]Cl lacks a carbonyl group, the acetylene conversion of [Hnmpi]Cl-0.67CuCl IL is merely 45.0%, which probably indicates the carbonyl group of [Hnmpo]Cl has an impact on the catalytic process. It should be highlighted that for all chlorocuprate(I) ILs, according to the results obtained by GC (Fig. S4), the selectivity for VCM is above 99%. The results of GC-MS confirm that the three by-products are dichloroethylene, dichloroethane, and 2-chloro-1,3-butadiene (Fig. S5). In short, the structure of organic chloride salt has a great effect on the catalytic performance of chlorocuprate(I) IL. Actually, the difference in catalytic performance is mainly caused by their different adsorption capacities for C_2H_2 and HCl, which will be further explained by theoretical calculations. Based on the above discussion, [Hnmpo]Cl-CuCl IL was selected for the subsequent studies.

3.2. Exploration of reaction conditions

The reaction conditions of acetylene hydrochlorination catalyzed by [Hnmpo]Cl-CuCl IL were explored to better understand the catalytic system. Firstly, it is necessary to investigate the influence of CuCl mole fraction.[50] However, when CuCl mole fraction in [Hnmpo]Cl-CuCl IL is above 0.67, a homogeneous liquid cannot be obtained even at 160 °C. Hence, we only studied the conditions that the CuCl mole fraction was less than or equal to 0.67, under which the mixture could exist in a liquid state below 100 °C. It can be seen in Fig. 3a that as the CuCl mole fraction increases from 0.33 to 0.60, the conversion of acetylene increases significantly from 78.7% to 89.0%, while the conversion decreases slightly to 87.9% with a further increase of CuCl mole fraction to 0.67. This decrease may be caused by the high viscosity of [Hnmpo]Cl-0.67CuCl IL (Fig. S6), which limits the mixing of reactants as well as the transfer of mass and heat. Meanwhile, we also see that the acetylene conversion is only 13.0% with [Hnmpo]Cl alone after 36 h of reaction, indicating a small contribution of [Hnmpo]Cl to the high catalytic activity of [Hnmpo]Cl-CuCl IL, and demonstrating that the main active component is Cu species. Taken together, these results show that the most appropriate CuCl mole fraction of [Hnmpo]Cl-CuCl IL is equal to 0.60.

GHSV is a crucial parameter in the gas phase reaction. Fig. 3b shows that the acetylene conversion slowly declines from 93.0% at 15 h^{-1} to 81.6% at 50 h^{-1}, because a higher GHSV results in lower residence time. However, the conversion of acetylene decreases very sharply as the further increase of GHSV. This drop can be partly ascribed to the transition of flow regime from bubble flow to churn turbulent flow or slug flow, which

generates large bubbles, yields smaller gas-liquid interfacial areas and therefore limits the mass transfer between the gas-liquid interface.[51] Even so, the conversion is as high as 52.0% at 180 h^{-1}. Consequently, [Hnmpo]Cl-0.60CuCl IL is a highly effective catalyst for acetylene hydrochlorination over a wide range of GHSV. Furthermore, we believe that designing a gas-liquid reactor with better mass transfer effect can still improve the catalytic performance.

As illustrated in Fig. 3c, with the increase of temperature from 120 to 180 °C, the acetylene conversion rises gradually from 77.0% to 91.0%, indicating that a higher temperature is capable of promoting reaction. A decline in the viscosity of [Hnmpo]Cl-0.60CuCl IL at higher temperatures is also conducive to the reaction (Fig. S6). However, at the temperature of 200 °C, the conversion decreases gradually as the time goes on, indicating too high a temperature is not a good choice and might increase the risk of the IL decomposition. Since the IL performs considerable activity and stability at a moderate temperature of 180 °C, then 180 °C is selected as the optimum temperature.

On one hand, excess acetylene could bring about rapid deactivation of catalyst and security concerns.[52, 53] On the other hand, HCl is helpful to maintain the stability of [Hnmpo]Cl-0.60CuCl IL, which will be discussed below in detail. Hence, a slight excess of HCl is required during the reaction process. However, excess HCl inevitably leads to an increase in the cost of production. Therefore, the effect of HCl/C_2H_2 volume ratio from 1.05 to 1.30 was discussed. Looking at Fig. 3d and S7, the acetylene conversion initially increases with the increase of HCl/C_2H_2 ratio. But when the HCl/C_2H_2 ratio is higher than 1.2, the conversion does not increase any more. As a result, the HCl/C_2H_2 volume ratio should be around 1.2.

3.3. Characterization of [Hnmpo]Cl-0.60CuCl IL

3.3.1. Thermal stability. TGA-DSC-FTIR were applied to study the thermal stability and decomposition products of [Hnmpo]Cl-0.60CuCl IL. Firstly, we can draw from the DSC curve in Fig. 4 that an endothermic peak appears at 84 °C, corresponding to the melting of the IL. Based on the TGA and DTG curves in Fig. 4, there are three distinct weight loss steps. When the temperature is 310 °C, the residual weight ratio is 52.7%, which matches well with the calculated CuCl weight ratio (52.3%). Meanwhile, another endothermic peak at 412 °C is in accordance with the melting of CuCl. Taken together, the main component at 310 °C is CuCl. Thus, the third weight loss above 481 °C is related to the vaporization of CuCl. According to the literature,[54, 55] the neutral NMPO and HCl may be present in [Hnmpo]Cl-0.60CuCl IL. As a result, a dynamic equilibrium is possible to exist: $[Hnmpo]^+Cl^-(l) \rightleftharpoons NMPO(l) + HCl(l) \rightleftharpoons NMPO(g) + HCl(g)$. At high temperature, [Hnmpo]Cl is easily volatilized as neutral molecular species by a proton transfer mechanism,

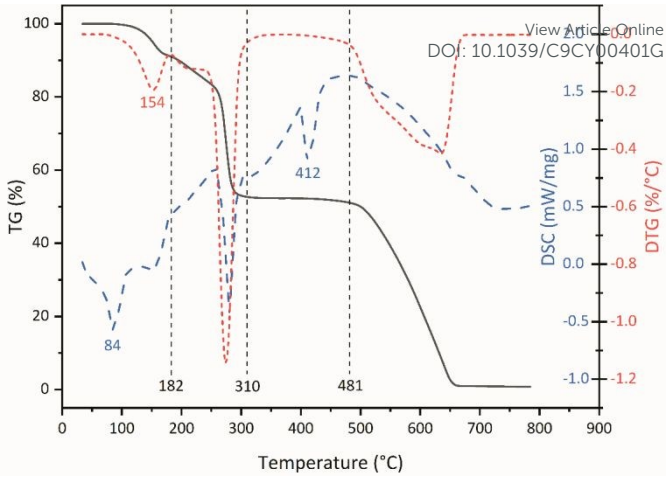

Fig. 4 TGA-DTG-DSC curves of [Hnmpo]Cl-0.60CuCl IL in N_2 atmosphere.

which can be supported by the results of simultaneously recorded FTIR spectra (Fig. S8). Therefore, the weight loss below 310 °C can be attributed to the vaporization of [Hnmpo]Cl. Moreover, according to the FTIR spectra of [Hnmpo]Cl and [Hnmpo]Cl-0.60CuCl IL in Fig. S9, we can infer that there is an interaction between [Hnmpo]Cl and CuCl in [Hnmpo]Cl-0.60CuCl IL, which might enhance the thermal stability of [Hnmpo]Cl. Hence, the first weight loss below 182 °C is probably due to the vaporization of free [Hnmpo]Cl that does not combine with CuCl, which can be further proved by the TGA result of pure [Hnmpo]Cl (Fig. S10).

Although in TGA curve the weight loss of [Hnmpo]Cl-0.60CuCl IL is up to 9.0% at 180°C, it is possible that extra HCl has the ability to inhibit the volatilization of [Hnmpo]Cl. Consequently, [Hnmpo]Cl-0.60CuCl IL would be more thermally stable with HCl introduction. Then, we performed long-term isothermal gravimetrical analyses to test this hypothesis (experimental details are shown in Fig. S11). The results display that the introduction of HCl profoundly impedes the volatilization of [Hnmpo]Cl, and [Hnmpo]Cl-0.60CuCl IL has only a small weight loss of about 3% at 180 °C in 24 h with continuous introduction of HCl, clearly indicating that the IL is thermally stable at 180 °C with HCl introduction.

In addition, ICP-OES was conducted to measure the Cu content in the fresh [Hnmpo]Cl-0.60CuCl IL, together with the used IL at 180 °C after 36 h of reaction. As summarized in Table 1, the Cu content of both ILs is similar to the nominal content, which demonstrates that there is a negligible loss of [Hnmpo]Cl after the reaction. Besides, the elemental composition of the fresh and the used ILs measured by XPS is shown in Table 1 and Fig. S12. As listed in Table 1, the relative Cu/N atomic ratio is 10.98 before the reaction. After the reaction, no drastic change in the Cu/N atomic ratio is occurred (11.05). Thus, XPS analysis

Table 1 The elemental composition and Cu content of the fresh and the used [Hnmpo]Cl-0.60CuCl ILs calculated from XPS and ICP-OES measurements.

Sample	The surface atomic composition of ILs (atom%)					Cu/N ratio	The content of Cu (wt%)	
	C 1s	O 1s	Cu 2p	Cl 2p	N 1s		Nominal	Actual
Fresh IL	28.08	6.25	27.67	35.48	2.52	10.98	33.53	33.44
Used IL	28.00	5.70	29.95	33.64	2.71	11.05	33.53	33.58

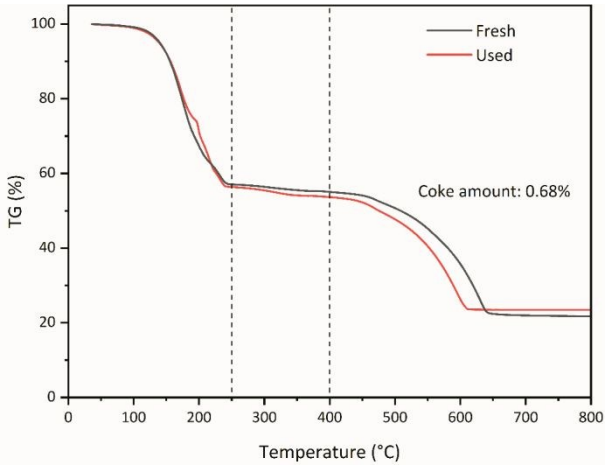

Fig. 5 TGA curves of the fresh and the used [Hnmpo]Cl-0.60CuCl ILs in air atmosphere.

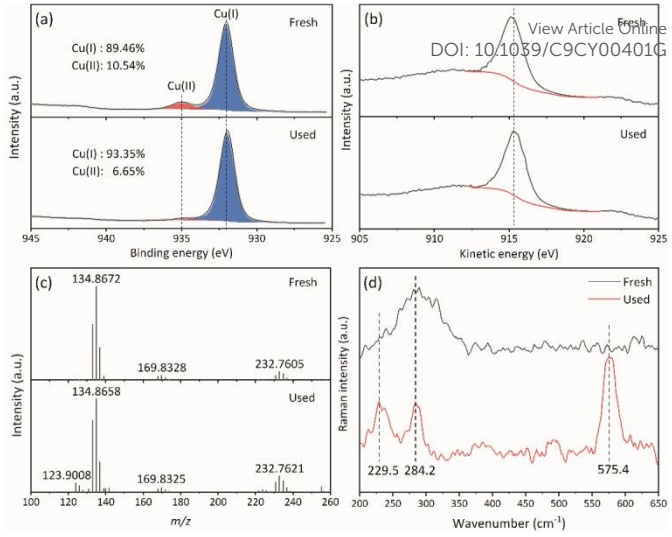

Fig. 6 (a) Cu 2p XPS, (b) Cu LMM Auger spectra, (c) ESI-MS at negative mode and (d) Raman spectra of the fresh and the used [Hnmpo]Cl-0.60CuCl ILs.

also shows that there is a negligible loss of [Hnmpo]Cl.

Overall, on the basis of these results, we therefore conclude that [Hnmpo]Cl-0.60CuCl IL has good thermal stability in the temperature ranges of 120−180 °C during the reaction.

3.3.2. Coke content. It is well-known that coke deposition, which may originate from acetylene, VCM, or their oligomers, is a common reason for the deactivation of solid catalysts in acetylene hydrochlorination.[52, 53] To measure the coke content, TGA was performed in air atmosphere. Fig. 5 shows the TGA results of the fresh [Hnmpo]Cl-0.60CuCl IL and the used IL at 30 h^{-1} GHSV after 36 h reaction. Based on the above discussion and previous literature,[56-59] we can infer that the weight loss caused by the coke formed in the reaction is mainly in the temperature range of 250–400 °C. In the case of the fresh IL, the weight loss is 2.03%, while it is 2.71% for the used IL. Thus, the content of coke in the used IL is estimated as low as 0.68%, which is far less than that of other solid catalysts under similar conditions,[12, 56, 57] and proves that coke is not easily formed in [Hnmpo]Cl-0.60CuCl IL. On the other side, unlike solid catalysts, the coke generated in liquid phase would not cover the active component, thereby further ensuring its long-term stability.

3.3.3. Valence state and speciation of copper. The change in the valence state of metal species during the reaction is also one of the main reasons for the deactivation of metal catalyst in acetylene hydrochlorination.[7, 52, 53] Therefore, to evaluate the valence state and speciation of copper in the fresh and the used [Hnmpo]Cl-0.60CuCl ILs, we applied an integrated approach combining XPS, UV-Vis, ESI-MS and Raman.

Fig. 6a shows the XPS spectra of Cu $2p_{3/2}$ core level for the fresh and used ILs, and the peaks were deconvoluted to distinguish the copper species and their relative quantities. The peak at 931.9 eV is related to the presence of Cu(I) or metallic Cu(0) species.[15] The other small peak with a higher binding energy of 935.0 eV is assigned to Cu(II) species,[15] perhaps because the raw material contained a small amount of Cu(II) or a small portion of Cu(I) was oxidized during the IL preparation process. As the binding energy of Cu $2p_{3/2}$ does not allow us to distinguish between Cu(I) and Cu(0), Cu LMM Auger spectra were measured. As illustrated in Fig. 6b, the presence of the peak at 915.3 eV and the absence of the peak at 918.0 eV suggest that there is only Cu(I) species but no metallic Cu(0) species in both ILs.[13, 14] Thus, the relative content of Cu(I) species in the fresh IL is 89.46%. After the reaction, the Cu(I) content even increases to 93.35%. And this change is consistent with the observation from UV-Vis spectra (Fig. S13), in which the absorbance intensity of Cu(II) species slightly decreases after the reaction. Overall, we could conclude Cu(I) species acts as the major active site in the reaction process. Besides, in combination with the results of acetylene conversion, the increase of Cu(I) species may also be one of the reasons for the slight enhancement of acetylene conversion after 36 h of reaction.

As shown in Fig. 6c, then the ILs are analyzed by ESI-MS at negative mode to identify the Cu species. For the fresh IL, the most intense peak is observed at *m/z* 134.9, corresponding to $CuCl_2^-$.[30] The second most intense peak corresponds to the dimer, $Cu_2Cl_3^-$, at *m/z* 232.8.[30] And another small peak at *m/z* 169.8 corresponds to $CuCl_3^-$. Compared with the fresh IL, the peaks of the used IL are basically unchanged, except for the appearance of several minor peaks that may be caused by reaction intermediates or by-products, indicating that the state of Cu species changes little. To our knowledge, acetylene can form a complex with Cu(I) as a π ligand.[60] After introducing HCl into the used IL for 2 h, we found the peak at *m/z* 123.9 nearly disappeared (Fig. S14). So it is reasonable to speculate that this peak corresponds to the CuCl-C_2H_2 π-complex, which could react with HCl, and demonstrating that acetylene can be activated by Cu(I) species in the IL.

Finally, we investigated the Raman spectral below 650 cm^{-1}, where the stretching vibrations of Cu−Cl are expected to be observed. Fig. 6d shows the Raman spectra of the fresh and the

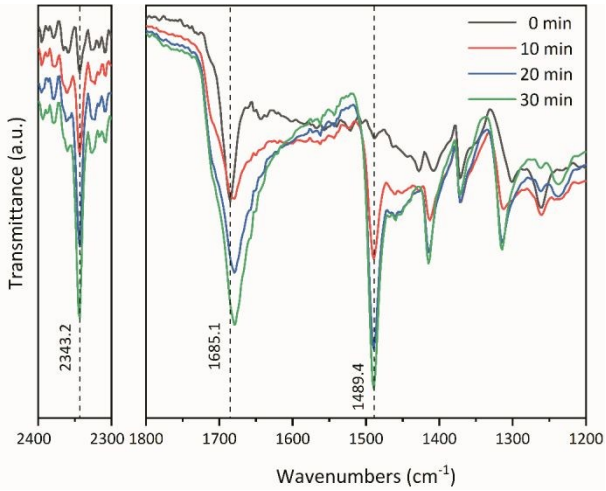

Fig. 7 *In situ* FTIR spectra of [Hnmpo]Cl-0.60CuCl IL in acetonitrile with continuous introduction of HCl. The absorption of pure acetonitrile was subtracted from the total absorption.

used ILs. It can be seen that the broad band around 284.2 cm^{-1} corresponds to the Cu−Cl vibration of the mixtures of $CuCl_2^-$ along with a minor amount of $Cu_2Cl_3^-$, as reported in the literature.[33, 61] Combined with the results of ESI-MS, the two new peaks appeared after the reaction might be assigned to the CuCl-C_2H_2 π-complex, the peak at 229.5 cm^{-1} belongs to the Cu−Cl vibration of CuCl,[62] and the peak at 575.4 cm^{-1} represents the C−H wagging vibration of C_2H_2.[63] Besides, we can hardly see the characteristic peaks of Cu(II) species in both of the ILs,[64] indicating Cu(I) species is indeed the main component and has not changed substantially after the reaction, which is consistent with the above results.

In brief, characterized by XPS, UV-Vis, ESI-MS and Raman, we confirm that the major valence state of copper in [Hnmpo]Cl-0.60CuCl IL is Cu(I), which is mainly $CuCl_2^-$ accompanied by a small amount of $Cu_2Cl_3^-$. And the Cu(I) species can maintain excellent stability during the reaction, thus the IL can keep catalytic activity for a long time.

3.3.4. Absorption and activation properties for reactant. According to previous research,[20, 29, 58] the adsorption properties of HCl and C_2H_2 on catalyst are critical in acetylene hydrochlorination. For one thing, the adsorption of HCl helps to improve the catalytic performance of catalyst, because the easy adsorption of HCl facilitates to react with C_2H_2 in a timely manner, and results in the decreasing of coke formation and metal reduction caused by excessive C_2H_2. For another, too strong adsorption of C_2H_2 is not conducive to the reaction, which may lead to fast deactivation of the catalyst.

As [Hnmpo]Cl could react with C_2H_2 to form VCM, we only discussed the absorption properties of pure NMPO toward individual HCl and C_2H_2. In reported literature,[65] 1 mol NMPO could absorb approximately 0.07 mol C_2H_2 under the conditions of 45 °C and 97 kPa. As a comparison, 1 mol NMPO could combine an equal amount of HCl to form [Hnmpo]Cl and still absorb a considerable amount of HCl.[24, 66] Of course, we can infer that C_2H_2 primarily combines with Cu(I) species when it is introduced into [Hnmpo]Cl-0.60CuCl IL. Additionally, the high

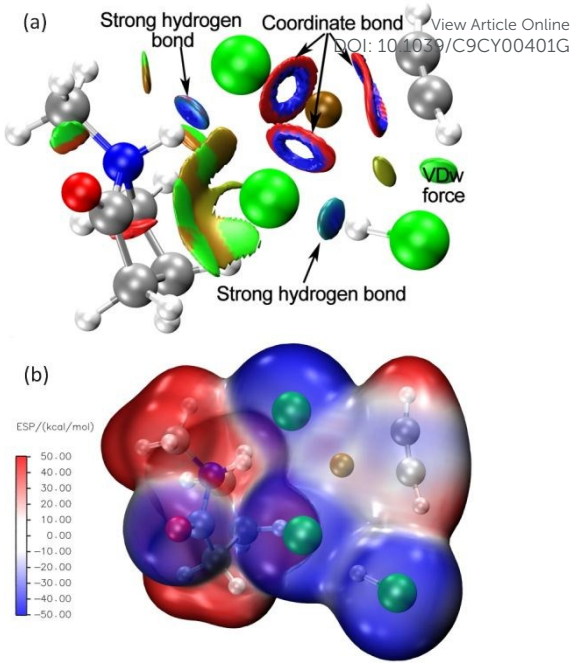

Fig. 8 (a) Plots of RDG isosurface for the structure of HCl and C_2H_2 both adsorbed by [Hnmpo][$CuCl_2$] (**Ad_C2H2_HCl**). Blue indicates strong attraction, green indicates very weak interaction, and red indicates strong repulsion. (b) The electrostatic potential mapped molecular ρ_e=0.0025 a.u. surface of **Ad_C2H2_HCl** structure.

solubility of HCl in NMPO is partly ascribed to the chemical interaction, indicating that the IL might have good activation ability for HCl.

To reveal the HCl activation mechanism, *in situ* FTIR analysis was carried to study the interaction between HCl and [Hnmpo]Cl-0.60CuCl IL. In the beginning, as can be seen from Fig. 7, the spectrum of the IL gave a band at 1685.1 cm^{-1}, which was attributed to the C=O stretching vibration. After HCl was introduced into the IL, the band appeared a red shift to 1679.5 cm^{-1} and its intensity gradually increased as time went on, which may be caused by the increasing interaction between HCl and the carbonyl group in N-methylpyrrolidonium cation. More importantly, two new bands appeared at 2343.2 cm^{-1} and 1489.4 cm^{-1}. The band at 2343.2 cm^{-1} was assigned to the H−Cl stretching vibration of HCl under the solvation of acetonitrile, which can be proven by the *in situ* FTIR spectra of acetonitrile with HCl introduction (Fig. S15). The other band at 1489.4 cm^{-1} should be attributed to the H−Cl stretching vibration of HCl interacted with the IL. This band demonstrated a nucleophilic effect in the activation of HCl *via* electron transfer process through the $^-$Cl···H−Cl strong hydrogen bond, which was visualized by using RDG method.[67] In Fig. 8a, the $^-$Cl···H−Cl hydrogen bond and the π-coordinate bond between C_2H_2 and Cu(I) are shown clearly. In addition, electrons of the IL can transfer through hydrogen bond, resulting in a decrease in the electrostatic potential of HCl molecule, which shows a nucleophilic activation mode (Fig. 8b). Obviously, the results discussed above confirm that HCl can be activated by the IL.

In short, the excellent HCl activation ability of [Hnmpo]Cl-0.60CuCl IL is beneficial to acetylene hydrochlorination, thus ensuring its great catalytic activity and stability.

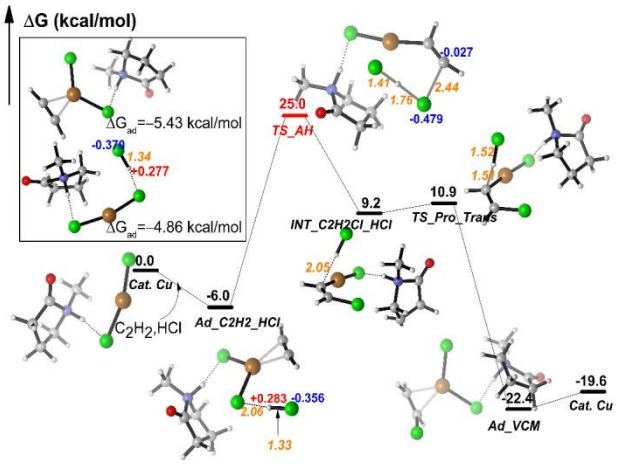

Fig. 9 The relative free energies (ΔG, in black numbers) are given in kcal/mol. The atom distance and NPA charges are represented in orange italic and red (or blue) numbers, respectively. Calculated at the M06-D3/SDD/6-311+G(2df,2p) level.

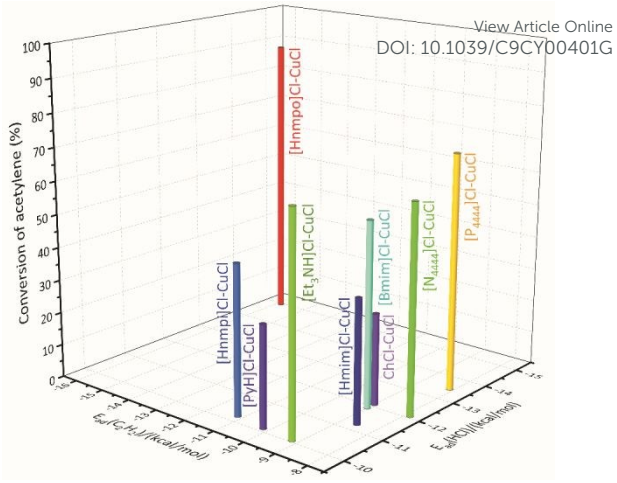

Fig. 10 Correlation of the catalytic performance with the adsorption energy of HCl and C_2H_2 in the range of ILs used.

3.4. Discussion of possible catalytic mechanism

Based on our experimental results, we combined the theoretical calculations to propose a possible catalytic mechanism of [Hnmpo]Cl-CuCl IL for acetylene hydrochlorination. When C_2H_2 and HCl are introduced into the IL, C_2H_2 preferentially combines with Cu(I) species to form π-complex, then the carbon-carbon triple bond of C_2H_2 is weakened, which means C_2H_2 has been activated. At the same time, HCl could also be adsorbed and activated by the IL. Therefore, [Hnmpo]Cl-CuCl IL is able to provide an efficient catalytic system for acetylene hydrochlorination. To further understand the reaction mechanism, DFT studies were carried out for acetylene hydrochlorination by using [Hnmpo][$CuCl_2$] as the catalyst, which is the most abundant Cu(I) species in this system.

In Fig. 9, the interaction between the catalyst and HCl or C_2H_2 was investigated first. The adsorption free energy of HCl and C_2H_2 on the catalyst is -4.86 kcal/mol and -5.43 kcal/mol. Although the adsorption capacity of the catalyst for HCl and C_2H_2 is almost equivalent, the forces of the interaction between C_2H_2 or HCl and catalyst are quite different, which are dominated by the π-coordinate and strong hydrogen bond, respectively. The π-coordinate causes the electron density of C_2H_2 molecule to decrease, therefore it shows the stronger electrophilic activity. Ingeniously, the formation of $^{-}$Cl···H–Cl hydrogen bond causes the electron transfer from the IL to HCl, and the NPA charge of HCl is negative, which enables HCl molecule to perform a nucleophilic process on the activated C_2H_2.

The mechanism of this addition reaction can be divided into two steps, which are the H–Cl cleaved to add Cl to C_2H_2 and proton transfer, respectively. The $\Delta G^{\neq}$ of **TS_AH** in the H–Cl cleavage step is the highest during the reaction process (25 kcal/mol), indicating that the addition of HCl to C_2H_2 is the key step of the whole reaction process, which is consistent with previous research.[29, 68, 69] In contrast, the $\Delta G^{\neq}$ of **TS_Pro_Trans** is only +10.9 kcal/mol, so it is a fast irreversible step for proton transfer. In addition, the desorption of VCM leads to +2.8 kcal/mol endergonic, so VCM is more negative than C_2H_2 (-5.43 kcal/mol) or HCl (-4.86 kcal/mol) to be adsorbed by the catalyst. Compared with traditional copper chlorides used for acetylene hydrochlorination, a significant feature of this chlorocuprate(I) IL is that more negative-charged ligands around the metal center, which may promote the nucleophilic addition of HCl to C_2H_2.

The theoretical evaluation of chlorocuprate(I) ILs used was performed to correlate the catalytic performance with the adsorption of C_2H_2 and HCl. Fig.10 shows that [Hnmpo]$CuCl_2$ has the strongest adsorption capacity for both C_2H_2 and HCl, and it has the best catalytic performance. Actually, the acetylene conversion appears to be more strongly correlated with the adsorption of HCl (Fig. S16), although it is not a complete linear correlation. So it can be proved that the adsorption of HCl is more critical to the reaction, which further supports the above-proposed mechanism. Moreover, for organic ammonium salts, the carbonyl group in [Hnmpo]$CuCl_2$ may improve the capacity of adsorbing reactants by increasing the energy of HOMO and reducing the energy of LUMO to a nicety (Table S2). A suitable orbital energy value can facilitate the adsorption and activation of reactants, thereby enhance its catalytic activity.

3.5. Long-term stability of [Hnmpo]Cl-0.60CuCl IL

From the perspective of industrial utilization, the long-term stability experiments of [Hnmpo]Cl-0.60CuCl IL were carried out under different acetylene GHSV at optimum reaction conditions (T = 180 °C, V(HCl)/V(C_2H_2) = 1.2), and the results were presented in Fig. 11. Surprisingly, the acetylene conversion did not decline over 150 h at 50 h^{-1} of industrial GHSV and even slightly increased from 82% to 86%. To further examine its durability, the IL was tested under a higher GHSV of 90 h^{-1}. As can be seen from Fig. 11, the initial acetylene conversion was 56% and then increased slightly, reaching a maximum of 60% at the reaction time of 60 h. After maintaining this conversion for about 30 h, the acetylene conversion slowly decreased to 53%, which was only a little lower than the initial value. Moreover, we characterized the IL after long-term reaction at 90 h^{-1} by

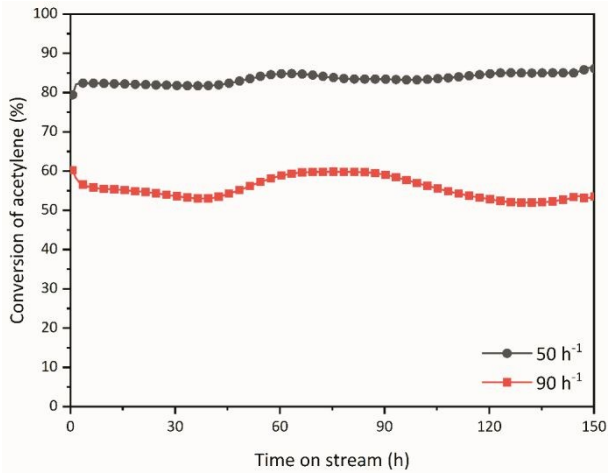

Fig. 11 Long-term stability of [Hnmpo]Cl-0.60CuCl IL. Reaction conditions: T = 180 °C and V(HCl)/V(C_2H_2) = 1.2.

TGA and ICP-OES. The TGA result demonstrates that the coke amount is only 1.34% (Fig. S17), illustrating that [Hnmpo]Cl-0.60CuCl IL possesses a strong ability to inhibit coke production. Additionally, the result of ICP-OES shows only a slight increase in Cu content after the long-term reaction (Table S3), reflecting the stability of [Hnmpo]Cl-0.60CuCl IL. Evidently, [Hnmpo]Cl-0.60CuCl IL is stable under typical conditions of acetylene hydrochlorination. These results obviously indicate that effective acetylene hydrochlorination can be accomplished with an inexpensive chlorocuprate(I) IL.

4. Conclusion

In summary, we reported a chlorocuprate(I) IL with excellent catalytic performance and superior stability in the gas-liquid acetylene hydrochlorination process. This is the first successful use of Cu(I) species as the main active component for acetylene hydrochlorination. At 180 °C and 30 h^{-1}, an acetylene conversion of 91% was obtained by using cost-efficient [Hnmpo]Cl-0.60CuCl IL. Besides, this IL had no visible decline in acetylene conversion even after 150 h of reaction at a high acetylene GHSV of 90 h^{-1}. Experimentally, the results of TGA-DSC-FTIR and ICP-OES demonstrated the IL was thermally stable under typical reaction conditions. The characterizations of XPS, UV-Vis, ESI-MS and Raman clearly showed that Cu(I) species was the major active component, and its valence state had hardly changed after the reaction. Additionally, the results obtained by *in situ* FTIR and theoretical calculations indicated that the IL could effectively adsorb and activate HCl to react with C_2H_2, which is the key feature of the IL that endow its outstanding catalytic performance. Overall, the reasons for the excellent catalytic activity and long-term stability of [Hnmpo]Cl-CuCl IL had been explained in detail. Therefore, our study proves chlorocuprate(I) IL can be a hopeful candidate for well-stabilized, low-cost, efficient and green non-mercury catalyst in the acetylene hydrochlorination, and also offers help for the future design of catalyst.

Conflicts of interest

There are no conflicts to declare.

View Article Online
DOI: 10.1039/C9CY00401G

Acknowledgements

The financial support from the National Basic Research Program of China (2012CB720302) and the National Key Research and Development Program of China (2016YFF0102503) are gratefully acknowledged.

Notes and references

1 R. Lin, A. P. Amrute and J. Pérez-Ramírez, *Chem. Rev.*, 2017, **117**, 4182-4247.
2 H. Xu and G. Luo, *J. Ind. Eng. Chem.*, 2018, **65**, 13-25.
3 United Nations Environment Programme, Minamata Convention on Mercury, http://www.mercuryconvention.org/, (accessed March 2018).
4 G. J. Hutchings, *J. Catal.*, 1985, **96**, 292-295.
5 B. Nkosi, N. J. Coville and G. J. Hutchings, *Appl. Catal.*, 1988, **43**, 33-39.
6 M. Conte, A. F. Carley, C. Heirene, D. J. Willock, P. Johnston, A. H. Herzing, C. J. Kiely and G. J. Hutchings, *J. Catal.*, 2007, **250**, 231-239.
7 X. Liu, M. Conte, D. Elias, L. Lu, D. J. Morgan, S. J. Freakley, P. Johnston, C. J. Kiely and G. J. Hutchings, *Catal. Sci. Technol.*, 2016, **6**, 5144-5153.
8 G. Malta, S. A. Kondrat, S. J. Freakley, C. J. Davies, L. Lu, S. Dawson, A. Thetford, E. K. Gibson, D. J. Morgan, W. Jones, P. P. Wells, P. Johnston, C. R. A. Catlow, C. J. Kiely and G. J. Hutchings, *Science*, 2017, **355**, 1399-1403.
9 K. Zhou, J. Jia, C. Li, H. Xu, J. Zhou, G. Luo and F. Wei, *Green Chem.*, 2015, **17**, 356-364.
10 J. Zhao, Y. Yu, X. Xu, S. Di, B. Wang, H. Xu, J. Ni, L. Guo, Z. Pan and X. Li, *Appl. Catal., B*, 2017, **206**, 175-183.
11 S. K. Kaiser, R. Lin, S. Mitchell, E. Fako, F. Krumeich, R. Hauert, O. V. Safonova, V. A. Kondratenko, E. V. Kondratenko, S. M. Collins, P. A. Midgley, N. López and J. Pérez-Ramírez, *Chem. Sci.*, 2019, **10**, 359-369.
12 J. Wang, W. Gong, M. Zhu and B. Dai, *Appl. Catal., A*, 2018, **564**, 72-78.
13 K. Zhou, J. Si, J. Jia, J. Huang, J. Zhou, G. Luo and F. Wei, *RSC Adv.*, 2014, **4**, 7766-7769.
14 J. Xu, J. Zhao, T. Zhang, X. Di, S. Gu, J. Ni and X. Li, *RSC Adv.*, 2015, **5**, 38159-38163.
15 H. Li, F. Wang, W. Cai, J. Zhang and X. Zhang, *Catal. Sci. Technol.*, 2015, **5**, 5174-5184.
16 Y. Zhai, J. Zhao, X. Di, S. Di, B. Wang, Y. Yue, G. Sheng, H. Lai, L. Guo, H. Wang and X. Li, *Catal. Sci. Technol.*, 2018, **8**, 2901-2908.
17 W. Zhao, M. Zhu and B. Dai, *Catal. Commun.*, 2017, **98**, 22-25.
18 D. Hu, L. Wang, F. Wang and J. Wang, *Chin. Chem. Lett.*, 2018, **29**, 1413-1416.
19 G. Qin, Y. Song, R. Jin, J. Shi, Z. Yu and S. Cao, *Green Chem.*, 2011, **13**, 1495-1498.
20 J. Hu, Q. Yang, L. Yang, Z. Zhang, B. Su, Z. Bao, Q. Ren, H. Xing and S. Dai, *ACS Catal.*, 2015, **5**, 6724-6731.
21 L. Yang, Q. Yang, J. Hu, Z. Bao, B. Su, Z. Zhang, Q. Ren and H. Xing, *AIChE J.*, 2018, **64**, 2536-2544.
22 J. Zhao, S. Gu, X. Xu, T. Zhang, Y. Yu, X. Di, J. Ni, Z. Pan and X. Li, *Catal. Sci. Technol.*, 2016, **6**, 3263-3270.

23 J. Zhao, Y. Yue, G. Sheng, B. Wang, H. Lai, S. Di, Y. Zhai, L. Guo and X. Li, *Chem. Eng. J.*, 2019, **360**, 38-46.
24 X. Zhou, S. Xu, Y. Liu and S. Cao, *Mol. Catal.*, 2018, **461**, 73-79.
25 H. Xu, S. Meng and G. Luo, *Catal. Sci. Technol.*, 2018, **8**, 1176-1182.
26 Y. Liu, R. Li, H. Sun and R. Hu, *J. Mol. Catal. A: Chem.*, 2015, **398**, 133-139.
27 B. Wiredu and A. S. Amarasekara, *Bioresour. Technol.*, 2015, **189**, 405-408.
28 X. Zhu, Y. Fu, H. Yin, A. Wang and X. Hou, *React. Kinet., Mech. Catal.*, 2016, **118**, 523-536.
29 H. Li, B. Wu, J. Wang, F. Wang, X. Zhang, G. Wang and H. Li, *Chin. J. Catal.*, 2018, **39**, 1770-1781.
30 C. Huang, B. Chen, J. Zhang, Z. Liu and Y. Li, *Energy Fuels*, 2004, **18**, 1862-1864.
31 S. E. Repper, A. Haynes, E. J. Ditzel and G. J. Sunley, *Dalton Trans.*, 2017, **46**, 2821-2828.
32 C. Chiappe, S. Rajamani and F. D'Andrea, *Green Chem.*, 2013, **15**, 137-143.
33 P. Gogoi, A. K. Dutta, P. Sarma and R. Borah, *Appl. Catal., A*, 2015, **492**, 133-139.
34 M. J. Frisch, G. W. Trucks, H. B. Schlegel, G. E. Scuseria, M. A. Robb, J. R. Cheeseman, G. Scalmani, V. Barone, B. Mennucci, G. A. Petersson, H. Nakatsuji, M. Caricato, X. Li, H. P. Hratchian, A. F. Izmaylov, J. Bloino, G. Zheng, J. L. Sonnenberg, M. Hada, M. Ehara, K. Toyota, R. Fukuda, J. Hasegawa, M. Ishida, T. Nakajima, Y. Honda, O. Kitao, H. Nakai, T. Vreven, J. A. Montgomery Jr., J. E. Peralta, F. Ogliaro, M. Bearpark, J. J. Heyd, E. Brothers, K. N. Kudin, V. N. Staroverov, R. Kobayashi, J. Normand, K. Raghavachari, A. Rendell, J. C. Burant, S. S. Iyengar, J. Tomasi, M. Cossi, N. Rega, J. M. Millam, M. Klene, J. E. Knox, J. B. Cross, V. Bakken, C. Adamo, J. Jaramillo, R. Gomperts, R. E. Stratmann, O. Yazyev, A. J. Austin, R. Cammi, C. Pomelli, J. W. Ochterski, R. L. Martin, K. Morokuma, V. G. Zakrzewski, G. A. Voth, P. Salvador, J. J. Dannenberg, S. Dapprich, A. D. Daniels, Ö. Farkas, J. B. Foresman, J. V. Ortiz, J. Cioslowski, and D. J. Fox, Gaussian 09 (Revision E.01), Gaussian Inc., Wallingford, CT, 2009.
35 C. Lee, W. Yang and R. G. Parr, *Phys. Rev. B*, 1988, **37**, 785-789.
36 A. D. Becke, *J. Chem. Phys.*, 1993, **98**, 5648-5652.
37 S. Grimme, S. Ehrlich and L. Goerigk, *J. Comput. Chem.*, 2011, **32**, 1456-1465.
38 S. Grimme, J. Antony, S. Ehrlich and H. Krieg, *J. Chem. Phys.*, 2010, **132**, 154104.
39 P. C. Hariharan and J. A. Pople, *Theor. Chim. Acta*, 1973, **28**, 213-222.
40 M. M. Francl, W. J. Pietro, W. J. Hehre, J. S. Binkley, M. S. Gordon, D. J. DeFrees and J. A. Pople, *J. Chem. Phys.*, 1982, **77**, 3654-3665.
41 P. J. Hay and W. R. Wadt, *J. Chem. Phys.*, 1985, **82**, 299-310.
42 A. E. Reed, R. B. Weinstock and F. Weinhold, *J. Chem. Phys.*, 1985, **83**, 735-746.
43 Y. Zhao and D. G. Truhlar, *Theor. Chem. Acc.*, 2008, **120**, 215-241.
44 P. Fuentealba, H. Preuss, H. Stoll and L. Von Szentpály, *Chem. Phys. Lett.*, 1982, **89**, 418-422.
45 A. D. McLean and G. S. Chandler, *J. Chem. Phys.*, 1980, **72**, 5639-5648.
46 R. Krishnan, J. S. Binkley, R. Seeger and J. A. Pople, *J. Chem. Phys.*, 1980, **72**, 650-654.
47 C. Y. Legault, CYLview, 1.0b, Université de Sherbrooke, 2009, http://www.cylview.org.
48 T. Lu and F. Chen, *J. Comput. Chem.*, 2012, **33**, 580-592.
49 W. Humphrey, A. Dalke and K. Schulten, *J. Mol. Graph.*, 1996, **14**, 33-38.
50 S. A. Bolkan and J. T. Yoke, *J. Chem. Eng. Data*, 1986, **31**, 194-197.
51 Y. T. Shah, B. G. Kelkar, S. P. Godbole and W. D. Deckwer, *AIChE J.*, 1982, **28**, 353-379.
52 B. Nkosi, N. J. Coville, G. J. Hutchings, M. D. Adams, J. Friedl and F. E. Wagner, *J. Catal.*, 1991, **128**, 366-377.
53 G. Malta, S. A. Kondrat, S. J. Freakley, C. Davies, S. Dawson, X. Liu, L. Lu, K. Dymkowski, F. Fernandez-Alonso, S. Mukhopadhyay, E. K. Gibson, P. P. Wells, S. F. Parker, C. J. Kiely and G. J. Hutchings, *ACS Catal.*, 2018, **8**, 8493-8505.
54 M. J. Earle, J. M. S. S. Esperança, M. A. Gilea, J. N. Canongia Lopes, L. P. N. Rebelo, J. W. Magee, K. R. Seddon and J. A. Widegren, *Nature*, 2006, **439**, 831-834.
55 T. L. Greaves and C. J. Drummond, *Chem. Rev.*, 2008, **108**, 206-237.
56 Z. Song, G. Liu, D. He, X. Pang, Y. Tong, Y. Wu, D. Yuan, Z. Liu and Y. Xu, *Green Chem.*, 2016, **18**, 5994-5998.
57 X. Li, J. Zhang and W. Li, *J. Ind. Eng. Chem.*, 2016, **44**, 146-154.
58 S. Shang, W. Zhao, Y. Wang, X. Li, J. Zhang, Y. Han and W. Li, *ACS Catal.*, 2017, **7**, 3510-3520.
59 H. Li, B. Wu, F. Wang and X. Zhang, *ChemCatChem*, 2018, **10**, 4090-4099.
60 Y. Tokita, A. Okamoto, K. Nishiwaki, M. Kobayashi and E. Nakamura, *Bull. Chem. Soc. Jpn.*, 2004, **77**, 1395-1399.
61 D. D. Axtell, B. W. Good, W. W. Porterfield and J. T. Yoke, *J. Am. Chem. Soc.*, 1973, **95**, 4555-4559.
62 G. Livescu, Z. Vardeny and O. Brafman, *Phys. Rev. B*, 1981, **24**, 1952-1960.
63 B. L. Chadwick and B. J. Orr, *J. Chem. Phys.*, 1992, **97**, 3007-3020.
64 K. Wang, F. Jian, R. Zhuang and H. Xiao, *Cryst. Growth Des.*, 2009, **9**, 3934-3940.
65 X. Huang and S. Li, *J. Chem. Eng. Data*, 2018, **63**, 2127-2134.
66 Z. Zhao, W. Qiao, Z. Li, G. Wang and L. Cheng, *J. Mol. Catal. A: Chem.*, 2004, **222**, 207-212.
67 E. R. Johnson, S. Keinan, P. Mori-Sánchez, J. Contreras-García, A. J. Cohen and W. Yang, *J. Am. Chem. Soc.*, 2010, **132**, 6498-6506.
68 Y. Han, M. Sun, W. Li and J. Zhang, *Phys. Chem. Chem. Phys.*, 2015, **17**, 7720-7730.
69 X. Li, Y. Nian, S. Shang, H. Zhang, J. Zhang, Y. Han and W. Li, *Catal. Sci. Technol.*, 2019, **9**, 188-198.

View Article Online
DOI: 10.1039/C9CY00401G

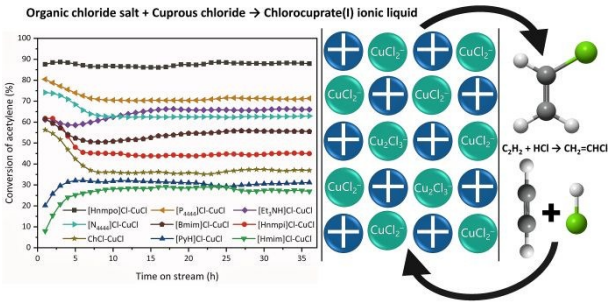

Chlorocuprate(I) ionic liquid can be a well-stabilized, low-cost, efficient and green non-mercury catalyst for hydrochlorination of acetylene.